Journal of Materials Chemistry C

Zero-Dimensional Metal Oxide Li4TiO4

Journal:	*Journal of Materials Chemistry C*
Manuscript ID	TC-ART-01-2019-000197.R1
Article Type:	Paper
Date Submitted by the Author:	20-Feb-2019
Complete List of Authors:	Du, Mao Hua ; Oak Ridge National Laboratory,

Zero-Dimensional Metal Oxide Li_4TiO_4

Mao-Hua Du

Materials Science and Technology Division, Oak Ridge National Laboratory, Oak Ridge, TN 37831, USA

Keywords: Li_4TiO_4; Luminescence; Exciton; Neutron scintillation; DFT calculation

Corresponding Author: Mao-Hua Du (mhdu@ornl.gov)

Abstract

Low-dimensional metal halides have recently emerged as promising luminescent materials; however, chemical and thermal instabilities of halides present challenges to their practical applications. In this paper, we show that low-dimensional metal oxides can exhibit efficient exciton emission based on hybrid functional calculations. We investigated a zero-dimensional ternary oxide, Li_4TiO_4, in which the anionic TiO_4 tetrahedra are spatially separated by highly electropositive Li cations that largely decouple the TiO_4 tetrahedra electronically. The resulting exciton self-trapping leads to the formation of Ti^{3+} and O_2^{3-} (V_k center) within a TiO_4 tetrahedron. The calculated strong exciton binding against dissociation to polarons/free carriers and giant Stokes shift indicate great potential of efficient luminescence at room temperature. We further suggest that Li_4TiO_4 should be a promising self-activated neutron scintillator due to the strong neutron absorption by Li and the efficient exciton emission. This work broadens the current research of low-dimensional metal-halide-based luminescent materials to include oxides with improved stability and new functionalities.

I. Introduction

Dimensional reduction is an effective tool for tuning optoelectronic properties for targeted functionalities in bulk semiconductors.[1-3] 2D atomic layers, 1D atomic chains, or 0D clusters can be incorporated within a bulk material, which exhibits properties resembling those of the low-dimensional components. Recently, low-dimensional metal halides have emerged as promising luminescent materials with potential applications in energy efficient lighting[4-10] and radiation detection [11] [12-14] thanks to the efficient emission by self-trapped excitons (STEs), which are stable at room temperature (RT) due to narrow electronic bands and soft crystal lattices. STE emission with high photoluminescence quantum efficiencies (PLQE) close to unity at RT has been reported in 0D hybrid organic-inorganic metal halides [e.g., $(C_4N_2H_{14}X)_4SnBr_6$, $(C_9NH_{20})_2SbCl_5$, $(Ph_4P)_2SbCl_5$ [8, 7]]. The crystal structure of 0D hybrid halides consists of inorganic metal halide anions, which are luminescent centers, and organic countercations that act as spacers between inorganic metal halide clusters. Such crystal structure leads to exciton localization at an isolated metal halide cluster and strong excited-state structural distortion. The resulting large Stokes shift suppresses energy transport between luminescent centers.[15] The formation of localized and immobile excitons in 0D metal halides is the key to the high PLQE observed in these materials.[16] All-inorganic 0D metal halides, in which anionic metal halide clusters are separated by inorganic countercations, have also been found to be excellent phosphors with high PLQE (e.g., $Cs_3Cu_2I_5$, Cs_4SnBr_6)[9, 10] and scintillators with high light yields under gamma ray irradiation [e.g., Cs_4EuX_6 (X = Br,I)][11]. Efficient STE emission at RT eliminates the need to introduce dopants for luminescence activation; thereby, simplifying phosphor/scintillator synthesis and avoiding potential problems that are often associated with

doping, such as low dopant solubility, formation of compensating defects, inhomogeneous dopant distribution, and phase segregation.

Previous works on low-dimensional luminescent materials have primarily focused on perovskite halides.[4, 5, 17] However, poor chemical and thermal stabilities of halides present challenges to their practical applications.[18] Phosphors used in commercial fluorescent and LED lamps (such as oxides and nitrides) must be stable in humid environment at elevated temperatures.[19-21] This work aims to obtain efficient STE emission in bulk oxides with reduced dimensionality based on first-principles materials design. Compared to metal halides that have relatively soft crystal lattices, the strong metal-oxide bonding in oxides increases the energy cost induced by the excited-state structural distortion that is associated with the STE formation. This limits the STE binding energy, resulting in thermal quenching of luminescence.[22] Dimensional reduction is expected to reduce the electronic band width and structural rigidness; thereby, increasing the STE binding energy in oxides. In this paper, we show hybrid functional calculations of excited-state structural and optical properties of Li_4TiO_4, a 0D oxide containing tetrahedral TiO_4 clusters. The results demonstrate the strong exciton self-trapping at TiO_4 anions and a giant Stokes shift of 3.47 eV, which indicate the potential for efficient luminescence. The high Li content and low density of Li_4TiO_4 further suggest that Li_4TiO_4 is a potential neutron scintillator material.

II. Computational Methods

All calculations on Li_4TiO_4 were based on density functional theory (DFT) implemented in the VASP code.[23] The interaction between ions and electrons was described by projector augmented wave method.[24] The kinetic energy cutoff of 520 eV was used for the plane-wave

basis. Li_4TiO_4 has a based-centered orthorhombic structure with space group *CmCm* (#63). Experimental lattice parameters (a = 5.4277 Å, b = 5.4277 Å, c = 6.1368 Å, α = 90°, β = 90°, γ = 93.5745°)[25] were used while the atomic positions were fully relaxed until the residual forces were less than 0.02 eV/ Å.

Electronic band structure and density of states (DOS) of Li_4TiO_4 were calculated using Perdew−Burke−Ernzerhof (PBE) exchange-correlation functional[26] while the exciton and polaron properties were treated by using more advanced hybrid PBE0 functional,[27] which has 25% non-local Fock exchange. A PBE calculation usually underestimates band gap while hybrid functional calculations (such as PBE0 and HSE) significantly improve the band gap description by partially correcting the self-interaction error.[27-29] The partial correction of the self-interaction error also leads to better description of charge localization and stability of hole/electron polarons and STE.[30-34] Between PBE0 and HSE functionals, the PBE0 band gap error is usually smaller in large-gap insulators but larger in semiconductors with medium to small band gaps.[29, 34, 35] We used PBE0 functional in this study because Li_4TiO_4 is an insulator with a large band gap (see Sec. III). The total energy of an exciton was calculated by fixing the occupation numbers of the electron and hole-occupied eigenlevels [Δ self-consistent field (ΔSCF) method[36-38]]. The ΔSCF method can be easily used in Li_4TiO_4 because the electron and hole are both localized on a single TiO_4 cluster and each occupies one single eigenlevel deep inside the band gap.[16] Such localized electron and hole levels are found for both unrelaxed and relaxed excitons. The ΔSCF method combined with the hybrid PBE0 functional allows excited-state structural relaxation and has shown accurate results in exciton excitation and emission energies in many compounds.[6, 8, 16, 34, 39-41]

Following the Franck-Condon principle, the exciton excitation and emission energies were obtained by calculating the total energy differences between the excited and the ground

states using PBE0-optimized ground-state and excited-state structures, respectively. The exciton binding energy relative to a free electron and a free hole was calculated by

$$\Delta B_{Ex} = E_0 + \varepsilon_g - E_{ex} \quad (2)$$

where E_0 and E_{ex} are the total energies of the defect-free supercell and the supercell that contains a relaxed exciton, respectively, and ε_g is the band gap. The hole polaron binding energy relative to a free hole is given by

$$\Delta B_{hole-pol} = E_0 - E_{hole-pol} - \varepsilon_{VBM} \quad (3)$$

while the electron polaron binding energy relative to a free electron is given by

$$\Delta B_{elec-pol} = \varepsilon_{CBM} - E_{elec-pol} + E_0 .^{34} \quad (4)$$

Here, $E_{hole-pol}$ and $E_{elec-pol}$ are the total energies of the supercells that contain a relaxed hole and electron polarons, respectively. ε_{VBM} and ε_{CBM} are the energies of the valence band maximum (VBM) and the conduction band minimum (CBM), respectively. With the results from Eqs. (2-4), the exciton binding energy relative to a hole and an electron polaron can then be calculated using

$$\Delta B_{Ex}^{pol} = \Delta B_{Ex} - \Delta B_{hole-pol} - \Delta B_{elec-pol} . \quad (5)$$

The image-charge and potential alignment corrections were applied to the total energies of the charged polarons.[42] The dielectric constant was calculated for the purpose of estimating the image charge correction. The calculated static dielectric constant is 14.14 (including both the electronic and ionic contributions).

III. Results and Discussion

The crystal structure of Li_4TiO_4 consists of anionic TiO_4 clusters separated by Li cations as shown in Figure 1. The calculated PBE band gap of Li_4TiO_4 is 4.64 eV, which is expected to be underestimated due to the well-known band gap error of the PBE calculation. The VBM is located at the Γ point while the CBM is localized between the Γ and the Y points [Figure 2(a)]. The more advanced hybrid PBE0 calculations increases the indirect band gap to 7.34 eV.

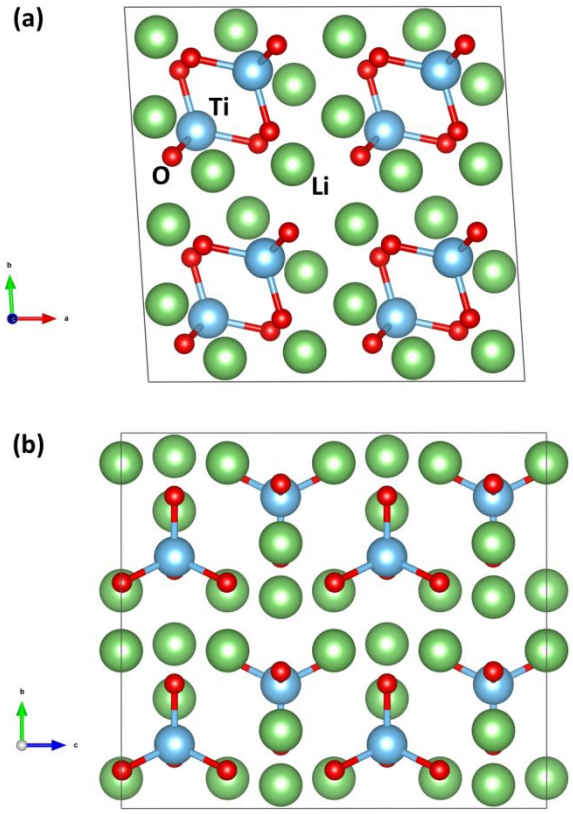

Figure 1. Crystal structure of Li_4TiO_4 viewed along (a) c and (b) a axes. Li, Ti, and O ions are represented by green, cyan, and red balls, respectively.

The calculated electronic band structure shows small dispersion for both conduction and valence bands [Figure 2(a)], which are primarily made up of Ti-3d and O-2p orbitals as shown in DOS [Figure 2(b)]. The flat conduction and valence bands are the result of the localized nature

of Ti-3d and O-2p orbitals and the Li spacers that further decouple the TiO_4 clusters. Li is much more electropositive than Ti; thus, the Li-2s orbital is much higher in energy than the Ti-3d orbital and has a very small contribution to the CBM. Both the conduction and the valence band states are distributed on weakly-coupled TiO_4 clusters; thereby, exhibiting the 0D character. The similar electronic structure can be found in 0D metal halides, such as Cs_4PbBr_6,[16] Cs_4SnBr_6,[43] and many double perovskite halides (such as $Cs_2NaInBr_6$), in which the cations with a relatively low electronegativity are spatially separated by highly electropositive cations.[44]

The small dispersion of both the valence and conduction bands in Li_4TiO_4 as shown in Figure 2(a) promotes charge localization. The PBE0 calculation shows that, without any structural distortion, the exciton is already localized at a TiO_4 cluster with a large binding energy of 1.43 eV (relative to a free electron and a free hole) calculated using Eq. 2. The electron is localized at the Ti cation while the hole is evenly distributed at the four adjacent O anions. The localization of the unrelaxed exciton is due to the strong Coulomb binding within a TiO_4 cluster and the narrow bands that results in a relatively small kinetic energy increase upon localization. The strong localization of exciton without structural distortion is a clear indication of the 0D nature of Li_4TiO_4.

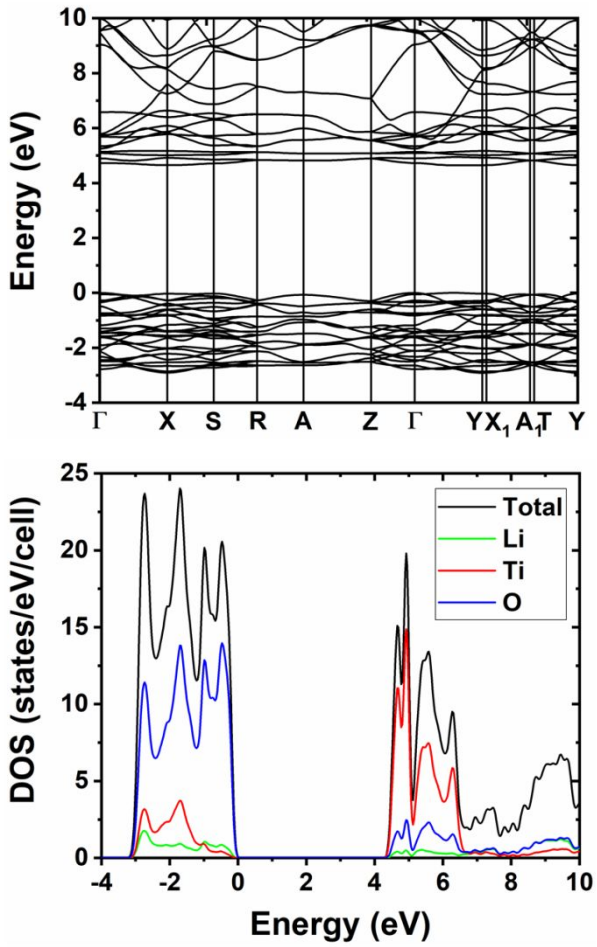

Figure 2. (a) Electronic band structure and (b) density of states (DOS) of Li_4TiO_4 calculated using the PBE functional. Note that the PBE band gap is underestimated.

Excited-state structural relaxation in the PBE0 calculation leads to strong structural distortion as shown in Figure 3. The two O ions move closer to form a O_2^{3-} (V_k center); the distance between the two O ions is reduced from 2.93 Å to 2.41 Å. The hole is localized on the anti-bonding orbital of O_2^{3-} [Figure 3(a)]. The formation of a V_k center is rare in oxides but common in halides because the chemical bonding in an oxide is usually much stronger than in halides, penalizing a substantial lattice distortion. However, in a 0D crystal structure, phonons are expected to be softened to allow the formation of a V_k center. The electron is localized at a Ti

ion [Figure 3(b)], forming Ti^{3+}. The exciton relaxation lowers the total energy by 1.38 eV, increasing the binding energy of a STE (relative to free carriers) to 2.81 eV. The binding energies of hole and electron polarons (relative to free carriers) were also calculated using Eqs. (3) and (4), yielding 0.36 eV and 1.02 eV, respectively. Thus, the STE binding energy relative to a hole and an electron polaron is 1.43 eV (Eq. 5). The above calculated large STE binding energies suggests that a STE is stable against dissociation into polarons/free carriers in Li_4TiO_4 at RT.

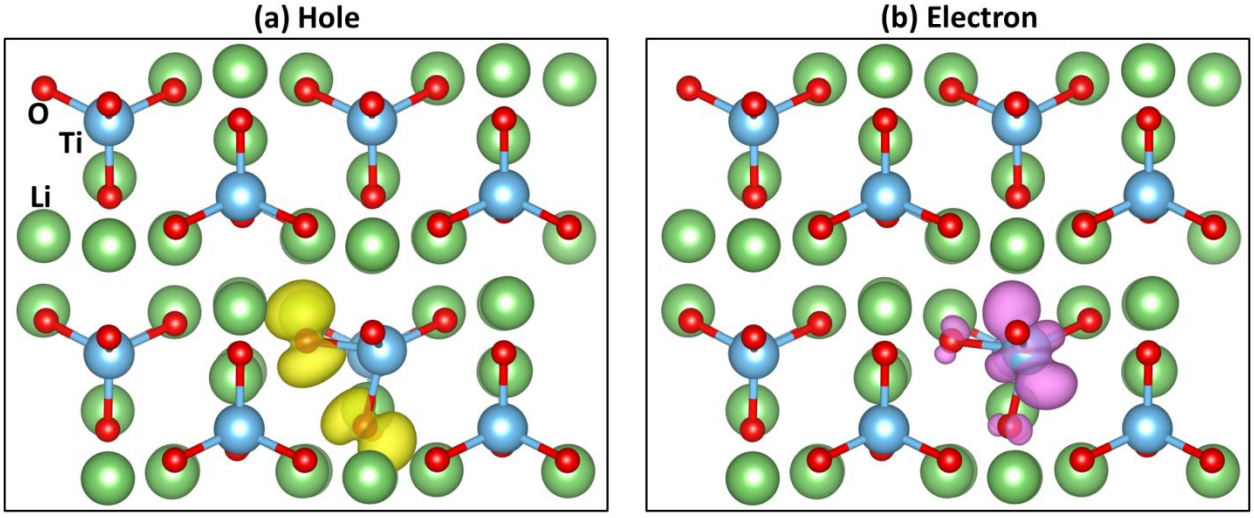

Figure 3. Isosurfaces of the partial charge density (0.005 e/bohr^3) of the hole (a) and the electron (b) in a self-trapped exciton in Li_4TiO_4. Li, Ti, and O ions are represented by green, cyan, and red balls, respectively.

The PBE0-calculated exciton excitation and emission energies in Li_4TiO_4 are shown in Table 1. We have also tested the hybrid HSE functional,[28, 29] which results in changes less than 0.01 eV in both excitation and emission energies. The calculated Stokes shift of 3.47 eV in Li_4TiO_4 is large compared to those found in 0D metal halides (< 2 eV).[17] A large Stokes shift is important for preventing self-absorption of luminescence as well as for reducing the efficiency of

exciton migration and the subsequent energy loss to defects.[15, 16] A large STE binding energy and a large Stokes shift in Li_4TiO_4 indicate efficient luminescence at RT because the former enhances radiative recombination and prevents thermal quenching of luminescence while the latter reduces nonradiative recombination.

Table 1. The calculated exciton excitation and emission energies in Li_4TiO_4 and Li_4SiO_4:Ti. The available experimental results[45] are shown in parentheses.

	Excitation Energy (eV)	Emission Energy (eV)	Stokes Shift (eV)
Li_4TiO_4	5.91	2.44	3.47
Li_4SiO_4:Ti	6.07 (6.20)	3.18 (3.54)	2.89 (2.66)

The high Li content renders Li_4TiO_4 a potential thermal neutron scintillator because ^6_3Li has a significant thermal neutron capture cross section of 940 barn.[46] Neutron scintillators are materials that emit photons under neutron irradiation. Coupling a neutron scintillator with a photodetector enables neutron detection, which has important applications including nonproliferation of special nuclear materials, homeland security, and various research instrumentation especially for detectors in neutron scattering experiments.[47] Li compounds have been extensively studied as thermal neutron scintillators.[47] Li_4TiO_4 has a high Li concentration of 4.43×10^{22} cm^{-3}. In comparison, LiI and Cs_2LiYCl_6, the two Li-containing solid-state neutron detector materials, have lower Li concentrations of 1.84×10^{22} cm^{-3} and 3.47×10^{21} cm^{-3}, respectively. As a result, Li_4TiO_4 should be more efficient in capturing thermal neutrons than LiI and Cs_2LiYCl_6. Li_4TiO_4 has a low density of 2.57 g/cm^3, significantly lower than those of LiI and

Cs_2LiYCl_6, which are 4.13 g/cm^3 and 3.33 g/cm^3, respectively. A low density is highly desirable for reducing sensitivity to background gamma rays.

The absorption of thermal neutrons by ^6_3Li leads to a nuclear reaction [$^6_3Li + {}^1_0n \rightarrow {}^4_2He$ (2.05 MeV) + ^3_1H (2.73 MeV)],[47] which produces secondary charged particles with significant energy. The radiation energy deposited into Li_4TiO_4 excites electrons and holes, which relax to the band edges to form STEs. The combination of strong thermal neutron absorption, relatively weak sensitivity to background gamma rays, and efficient STE emission at RT indicate potential application of Li_4TiO_4 as an efficient thermal neutron scintillator material.

The excitation and emission energies of an exciton bound to a substitutional Ti_{Si} dopant in Li_4SiO_4:Ti were calculated and the results are compared with the experimental values in Table 1. The excellent agreement between the calculated and measured results shows that the PBE0 calculation gives accurate descriptions of excitation, excited-state structural relaxation, and emission and that the theoretical prediction of the excited properties in Li_4TiO_4 is reliable. It is interesting to note that the structural distortion induced by a bound exciton in Li_4SiO_4:Ti (Figure 4) is different from that by a STE in Li_4TiO_4 (Figure 3). In Li_4SiO_4:Ti, the exciton localization at Ti_{Si} does not lead to the formation of a V_k center in contrast to the STE in Li_4TiO_4. Instead, the hole in the bound exciton in Li_4SiO_4:Ti is localized at a single O ion, as shown in Figure 4(a), which, in turn, causes the elongation of the Ti-O bond. Ti^{4+} has a larger size than Si^{4+}. (The ionic radii of four-fold coordinated Ti^{4+} and Si^{4+} ions are 0.42 Å and 0.26 Å, respectively.) As such, the substitution of Si^{4+} by Ti^{4+} applies a compressive strain to the surrounding crystal lattice, which prevents the strong structural distortion associated with the V_k formation. Consequently, the calculated Stokes shift in Li_4SiO_4:Ti (2.89 eV) is significantly lower than that in Li_4TiO_4 (3.47 eV). As a self-activated scintillator, the exciton localization after excitation in Li_4TiO_4 does

not require transport of excitation energy to activators; thereby, further reducing the probability of energy loss to defects. It is, thus, expected that Li_4TiO_4 should be a more efficient neutron scintillator than Li_4SiO_4:Ti.

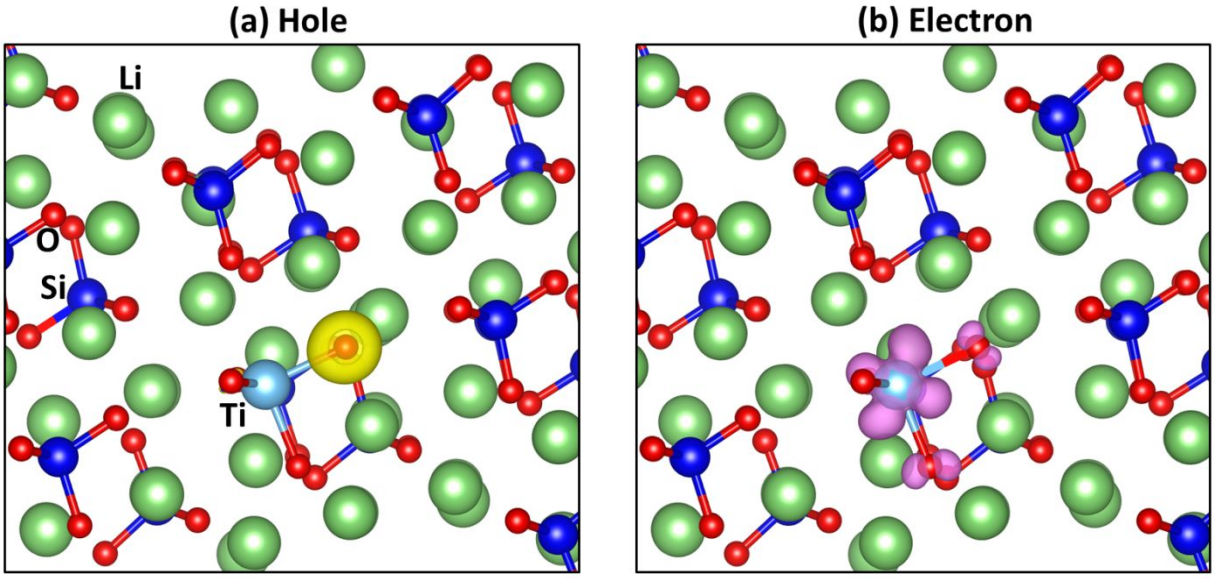

Figure 4. Isosurfaces of the partial charge density (0.005 e/bohr^3) of the hole (a) and the electron (b) in an exciton trapped by a substitutional dopant Ti_{Si} in Li_4SiO_4. Li, Si, Ti, and O ions are represented by green, blue, cyan, and red balls, respectively.

IV. Conclusions

Hybrid DFT calculations reveal novel photophysical properties of a 0D ternary metal oxide, Li_4TiO_4. The calculated large STE binding energy and giant Stokes shift in Li_4TiO_4 indicate the potential of RT luminescence with high quantum efficiency. These properties are the direct result of the 0D structure, in which the anionic TiO_4 tetrahedra are spatially separated by highly electropositive Li cations that largely decouple the TiO_4 tetrahedra electronically. The efficient STE emission combined with strong thermal neutron absorption by Li indicate the promise of Li_4TiO_4 as an efficient self-activated thermal neutron scintillator. Future research on

tuning the band gap and electron-phonon coupling should expand the functionalities and applications of low-dimensional oxides.

ACKNOWLEDGMENTS

We are grateful for the useful discussion with David Mandrus and Zane W. Bell. This work was supported by the ORNL Seed Money Fund.

References:

1. E. G. Tulsky and J. R. Long, *Chemistry of Materials*, 2001, **13**, 1149-1166.
2. J. Androulakis, S. C. Peter, H. Li, C. D. Malliakas, J. A. Peters, Z. Liu, B. W. Wessels, J.-H. Song, H. Jin, A. J. Freeman and M. G. Kanatzidis, *Advanced Materials*, 2011, **23**, 4163-4167.
3. B. Saparov and D. B. Mitzi, *Chemical Reviews*, 2016, **116**, 4558-4596.
4. H. Lin, C. Zhou, Y. Tian, T. Siegrist and B. Ma, *ACS Energy Letters*, 2018, **3**, 54-62.
5. M. D. Smith and H. I. Karunadasa, *Accounts of Chemical Research*, 2018, **51**, 619-627.
6. C. Zhou, H. Lin, Q. He, L. Xu, M. Worku, M. Chaaban, S. Lee, X. Shi, M.-H. Du and B. Ma, *Materials Science and Engineering: R: Reports*, 2019, **137**, 38-65.
7. C. Zhou, H. Lin, Y. Tian, Z. Yuan, R. Clark, B. Chen, L. J. van de Burgt, J. C. Wang, Y. Zhou, K. Hanson, Q. J. Meisner, J. Neu, T. Besara, T. Siegrist, E. Lambers, P. Djurovich and B. Ma, *Chemical Science*, 2018, **9**, 586-593.
8. C. Zhou, M. Worku, J. Neu, H. Lin, Y. Tian, S. Lee, Y. Zhou, D. Han, S. Chen, A. Hao, P. I. Djurovich, T. Siegrist, M.-H. Du and B. Ma, *Chemistry of Materials*, 2018, **30**, 2374-2378.
9. B. M. Benin, D. N. Dirin, V. Morad, M. Wörle, S. Yakunin, G. Rainò, O. Nazarenko, M. Fischer, I. Infante and M. V. Kovalenko, *Angewandte Chemie International Edition*, 2018, **57**, 11329-11333.
10. T. Jun, K. Sim, S. Iimura, M. Sasase, H. Kamioka, J. Kim and H. Hosono, *Advanced Materials*, 2018, **30**, 1804547.
11. Y. Wu, D. Han, B. C. Chakoumakos, H. Shi, S. Chen, M.-H. Du, I. Greeley, M. Loyd, D. J. Rutstrom, L. Stand, M. Koschan and C. L. Melcher, *Journal of Materials Chemistry C*, 2018, **6**, 6647-6655.
12. L. A. Boatner, D. Wisniewski, J. S. Neal, J. O. Ramey, J. A. Kolopus, B. C. Chakoumakos, M. Wisniewska and R. Custelcean, *Applied Physics Letters*, 2008, **93**, 244104.
13. S. A. Vaughn, B. C. Chakoumakos, R. Custelcean, J. O. Ramey, M. D. Smith, L. A. Boatner and H.-C. zur Loye, *Inorganic Chemistry*, 2012, **51**, 10503-10511.
14. R. Roccanova, W. Ming, V. R. Whiteside, M. A. McGuire, I. R. Sellers, M.-H. Du and B. Saparov, *Inorganic Chemistry*, 2017, **56**, 13878-13888.
15. G. Blasse and B. C. Grabmaier, *Luminescent Materials*, Springer-Verlag, Berlin Heidelberg, 1994.
16. D. Han, H. Shi, W. Ming, C. Zhou, B. Ma, B. Saparov, Y.-Z. Ma, S. Chen and M.-H. Du, *Journal of Materials Chemistry C*, 2018, **6**, 6398-6405.

17. C. Zhou, H. Lin, Q. He, L. Xu, M. Worku, M. Chaaban, S. Lee, X. Shi, M.-H. Du and B. Ma, *Materials Science & Engineering R-Reports*, 2019, **137**, 38-65.
18. X. Zhao and N.-G. Park, *Photonics*, 2015, **2**, 1139.
19. A. M. Srivastava and T. J. Sommerer, *ECS INTERFACE*, 1998, **2**, 28.
20. J. McKittrick and L. E. Shea-Rohwer, *Journal of the American Ceramic Society*, 2014, **97**, 1327-1352.
21. J. Meyer and F. Tappe, *Advanced Optical Materials*, 2015, **3**, 424-430.
22. K. Tanimura and L. E. Halliburton, *Physical Review B*, 1986, **34**, 2933-2935.
23. G. Kresse and J. Furthmüller, *Computational Materials Science*, 1996, **6**, 15-50.
24. G. Kresse and D. Joubert, *Physical Review B*, 1999, **59**, 1758.
25. R. P. Gunawardane, J. G. Fletcher, M. A. K. L. Dissanayake, R. A. Howie and A. R. West, *Journal of Solid State Chemistry*, 1994, **112**, 70-72.
26. J. P. Perdew, K. Burke and M. Ernzerhof, *Physical review letters*, 1996, **77**, 3865.
27. J. P. Perdew, M. Emzerhof and K. Burke, *Journal of Chemical Physics*, 1996, **105**, 9982-9985.
28. J. Heyd, G. E. Scuseria and M. Ernzerhof, *Journal of Chemical Physics*, 2003, **118**, 8207-8215.
29. J. Paier, M. Marsman, K. Hummer, G. Kresse, I. C. Gerber and J. G. Angyan, *Journal of Chemical Physics*, 2006, **124**.
30. M.-H. Du and S. B. Zhang, *Physical Review B*, 2009, **80**, 115217.
31. A. Janotti, J. B. Varley, M. Choi and C. G. Van de Walle, *Physical Review B*, 2014, **90**, 085202.
32. A. Janotti, C. Franchini, J. B. Varley, G. Kresse and C. G. Van de Walle, *physica status solidi (RRL) – Rapid Research Letters*, 2013, **7**, 199-203.
33. L. Bjaalie, D. G. Ouellette, P. Moetakef, T. A. Cain, A. Janotti, B. Himmetoglu, S. J. Allen, S. Stemmer and C. G. V. d. Walle, *Applied Physics Letters*, 2015, **106**, 232103.
34. K. Biswas and M. H. Du, *Physical Review B*, 2012, **86**, 014102.
35. A. J. Garza and G. E. Scuseria, *The Journal of Physical Chemistry Letters*, 2016, **7**, 4165-4170.
36. R. O. Jones and O. Gunnarsson, *Reviews of Modern Physics*, 1989, **61**, 689-746.
37. A. Görling, *Physical Review A*, 1999, **59**, 3359-3374.
38. A. Hellman, B. Razaznejad and B. I. Lundqvist, *The Journal of Chemical Physics*, 2004, **120**, 4593-4602.
39. C. Zhou, H. Lin, H. Shi, Y. Tian, C. Pak, M. Shatruk, Y. Zhou, P. Djurovich, M.-H. Du and B. Ma, *Angewandte Chemie International Edition*, 2018, **57**, 1021.
40. G. Wu, C. Zhou, W. Ming, D. Han, S. Chen, D. Yang, T. Besara, J. Neu, T. Siegrist, M.-H. Du, B. Ma and A. Dong, *ACS Energy Letters*, 2018, **3**, 1443-1449.
41. X. Wang, W. Meng, W. Liao, J. Wang, R.-G. Xiong and Y. Yan, *The Journal of Physical Chemistry Letters*, 2019, **10**, 501-506.
42. S. Lany and A. Zunger, *Physical Review B*, 2008, **78**, 235104.
43. H. Shi, D. Han, S. Chen and M.-H. Du, *submitted.*
44. H. L. Shi and M. H. Du, *Phys. Rev. Appl.*, 2015, **3**, 054005.
45. J. Pejchal, V. Babin, A. Beitlerova, S. Kurosawa, Y. Yokota, A. Yoshikawa and M. Nikl, *Journal of Crystal Growth*, 2017, **457**, 143-150.
46. V. F. Sears, *Neutron News*, 1992, **3**, 26-37.
47. A. N. Caruso, *Journal of Physics: Condensed Matter*, 2010, **22**, 443201.